Renoprotective Effect of Combined Inhibition of Angiotensin-Converting Enzyme and Histone Deacetylase

Yifei Zhong,*† Edward Y. Chen,‡§ Ruijie Liu,*¶ Peter Y. Chuang,* Sandeep K. Mallipattu,* Christopher M. Tan,‡§ Neil R. Clark,‡§ Yueyi Deng,† Paul E. Klotman,‖ Avi Ma'ayan,‡§ and John Cijiang He*‡¶

*Department of Medicine, Mount Sinai School of Medicine, New York, New York; †Department of Nephrology, Longhua Hospital, Shanghai University of Traditional Chinese Medicine, Shanghai, China; ‡Department of Pharmacology and Systems Therapeutics and §Systems Biology Center New York, Mount Sinai School of Medicine, New York, New York; ‖Baylor College of Medicine, Houston, Texas; and ¶Renal Section, James J. Peters Veterans Affairs Medical Center, New York, New York

ABSTRACT

The Connectivity Map database contains microarray signatures of gene expression derived from approximately 6000 experiments that examined the effects of approximately 1300 single drugs on several human cancer cell lines. We used these data to prioritize pairs of drugs expected to reverse the changes in gene expression observed in the kidneys of a mouse model of HIV-associated nephropathy (Tg26 mice). We predicted that the combination of an angiotensin-converting enzyme (ACE) inhibitor and a histone deacetylase inhibitor would maximally reverse the disease-associated expression of genes in the kidneys of these mice. Testing the combination of these inhibitors in Tg26 mice revealed an additive renoprotective effect, as suggested by reduction of proteinuria, improvement of renal function, and attenuation of kidney injury. Furthermore, we observed the predicted treatment-associated changes in the expression of selected genes and pathway components. In summary, these data suggest that the combination of an ACE inhibitor and a histone deacetylase inhibitor could have therapeutic potential for various kidney diseases. In addition, this study provides proof-of-concept that drug-induced expression signatures have potential use in predicting the effects of combination drug therapy.

J Am Soc Nephrol 24: 801–811, 2013. doi: 10.1681/ASN.2012060590

Treatment options for kidney diseases that display fibrosis are limited, and combination therapy is expected to be more effective because of the disease complexity. For example, the combination of angiotensin-converting enzyme inhibitors (ACEIs) with angiotensin-receptor blockers (ARBs),[1] renin inhibitors with ACEIs,[2] and aldosterone inhibitors with ACEIs[3,4] are expected to provide better renal protection than use of these drugs as monotherapies. However, large clinical trials demonstrated that these combination therapies lead to more harmful adverse events than beneficial effects.[5–8] Combination therapies are mostly based on intuitive clinical experience and often target the same molecular pathways (*e.g.*, the renin-angiotensin II system). Such approaches commonly aggravate adverse effects, as evidenced by recent clinical trials.[9]

Received June 19, 2012. Accepted January 9, 2013.

Y.Z. and E.Y.C. contributed equally to this work.

Published online ahead of print. Publication date available at www.jasn.org.

Correspondence: Dr. John Cijiang He (experimental part), Department of Medicine, Division of Nephrology, Mount Sinai School of Medicine, One Gustave L. Levy Place, Box 1243, New York, NY 10029, or Dr. Avi Ma'ayan (computational part), Department of Pharmacology and Systems Therapeutics, One Gustave L. Levy Place, Box 1215, Mount Sinai School of Medicine, New York, NY 10029. Email: cijiang.he@mssm.edu, avi.maayan@mssm.edu

A rational approach to predict combinations of drugs for better protection from kidney injury is urgently needed. Systems pharmacology, a new and emerging offshoot of systems biology, is aiming to link genome-wide measurements and biological networks with the effects of drugs on cells, tissues, and organisms to accelerate the discovery of new biomarker sets, drug targets, drugs, drug combinations, and prediction of adverse and desired drug-induced effects in individual patients.[10]

One of the early and seminal contributions to the field of systems pharmacology was a large-scale study conducted at the Broad Institute called the Connectivity Map (CMAP).[11] In this study, approximately 6000 genome-wide mRNA microarray experiments were performed using human cancer cell lines, 6 hours after exposure to approximately 1300 individual drugs, many of them Food and Drug Administration (FDA) approved, in different concentrations. The idea behind the CMAP study is revolutionary for drug discovery because it promotes a signature-based drug profiling approach, avoiding the need for details about the specifics of drug targets or even knowledge of the targeted pathways.[12]

The CMAP website provides access to all experimental data for download, as well as a web-based tool to query the database for drugs and experiments that match user input lists of up and down differentially expressed genes. For this study, we implemented a different algorithm to match user-provided lists of differentially expressed genes with drug-induced signatures from CMAP. Our method searches for combinations of drugs instead of single drugs. The method searches for a pair of drugs that can theoretically maximally flip the expression of genes that are downregulated or upregulated in the disease on the basis of the effects of those drugs on gene expression in cells from CMAP. To achieve this, we first extracted the 500 genes that are most upregulated or most downregulated by each experiment in CMAP. Given as input two gene lists (down- or upregulated genes in the disease), we exhaustively searched for pairs of drugs that upregulate the downregulated genes in the disease and downregulate the upregulated genes in the disease, with minimally upregulating genes that are already listed as up, or downregulating genes that changed in the down direction.

Using this approach, we determined potential drug combinations that could reverse the maximal number of genes altered in the kidneys of HIV-1 transgenic mice (Tg26), a model for HIV-associated nephropathy (HIVAN), compared with their wild-type littermates.[13] The method predicted that the combination of an ACEI with a histone deacetylase inhibitor (HDACI) could reverse the maximal number of genes altered in Tg26 kidneys. To examine the validity of this prediction, we experimentally confirmed that ACEI and HDACI together provide additive renal protection in Tg26 mice. In addition, we further confirmed that the genes predicted to be flipped by the drug combination are indeed altered after drug treatment.

RESULTS

Prediction of Drug Combinations That Could Reverse Gene Expression Altered in Tg26 Kidneys

To process the microarray gene expression from CMAP, we first downloaded the ranked gene list table from http://www.broadinstitute.org/cmap/ and extracted the top and bottom 500 genes from each experiment to generate two gene set libraries (one for upregulated genes and the other for downregulate genes). Each library consists of approximately 6000 rows, with each row containing lists of 500 most upregulated or downregulated genes for each experiment from CMAP. The analysis of gene expression microarrays obtained from kidneys of Tg26 mice compared with their wild-type littermates identified 1057, or 434, upregulated genes, and 413, or 72, downregulated genes on the basis of two different threshold criteria, respectively. The first and the less stringent criterion was a *P* value of 0.01 without the Benjamini-Hochberg correction, and the second criterion was a q-value of 0.1, which includes the Benjamini-Hochberg correction. These microarray data were deposited into National Center for Biotechnology Information (NCBI)'s Gene Expression Omnibus GEO record number GSE35226.[13] Supplemental Tables 1 and 2 list the differentially expressed genes with their expression levels.

We then assessed the overlap among these gene lists with the two gene set libraries created from CMAP to identify the top pairs of drugs (Table 1 and Supplemental Table 3). Using equation 1 described in detail in the Concise Methods section, we ranked pairs of drugs that can maximally reverse the differentially expressed genes in Tg26 mice. To match human and mouse genes, we used NCBI's homologene. The method is made available for general use to identify drug pairs for other diseases or for any similar experimental settings. We developed the software tool Drug Pair Seeker (DPS) which can be used to perform the analysis on any sets of mammalian up- and downregulated genes. DPS, implemented in Java, is cross-platform independent and can be accessed at http://www.maayanlab.net/DPS.

Using this approach, we found that the ACEI (captopril) and HDACIs (trichostatin A or vorinostat) received high scores and are among the top 10 combinations that are predicted to maximally reverse the genes differentially expressed in Tg26 mice under both threshold criteria (Table 1 and Supplemental Table 3). Captopril, an ACEI, has been widely used to treat patients with kidney diseases,[14] whereas trichostatin A or vorinostat, which are both HDACIs, have been recently shown to improve the status of kidney fibrosis in animal models of kidney diseases;[15] thus, we decided to focus on these two drugs. On the basis of our prior clinical and pharmacological understanding, other combinations among the top 10 are less likely to have renal protection, so we did not pursue them first. Furthermore, because some evidence already suggests that these two classes of drugs could potentially work individually, we decided to select ACEI and HDACI for further validation in combination. Our prediction is that captopril would

Table 1. Identification of drug combination by using computational prediction

Drug 1	Drug 2	Total Coverage	Total Conflicts	Drug 1 Coverage	Drug 1 Conflicts	Drug 2 Coverage	Drug 2 Conflicts
Trichostatin A-6193	Lansoprazole-2967	117	44	70	22	53	24
Trichostatin A-6193	Betulinic acid-1345	113	42	70	22	47	20
Trichostatin A-6193	Tolnaftate-2001	118	48	70	22	52	28
Vorinostat-6179	Lansoprazole-2967	117	47	66	25	53	24
Trichostatin A-6193[a]	Captopril-1988	119	51	70	22	51	31
Trichostatin A-6193	Trapidil-3136	113	45	70	22	47	24
Trichostatin A-6193	Fulvestrant-6918	116	48	70	22	47	29
Trichostatin A-6193	Meteneprost-7552	111	43	70	22	46	22
Trichostatin A-6193	Verapamil-1927	112	45	70	22	46	25
Trichostatin A-1175	Betulinic acid-1345	104	37	58	18	47	20

Top 10 computationally predicted combination of drugs using the less stringent criteria of ANOVA with $P<0.01$ without the Benjamini-Hochberg correction for determining differentially expressed genes in HIVAN from Tg26 mice. The numbers next to each drug name represents the specific experiment number from CMAP. This number can be used for finding more information about the CMAP experiment, such as cell type, concentration, and microarray platform. "Coverage" means the number of genes the drug potentially flips in the right direction, and "conflicts" means the number of genes the drug is potentially changing in the undesired direction. Trichostatin A is an HDAC inhibitor; lansoprazole is a proton-pump inhibitor; betulinic acid is an apoptosis inducer and an anti-cancer agent; tolnaftate is an antifungal; captopril is an ACE inhibitor; trapidil is a vasodilator and an antiplatelet agent; fulvestrant is an estrogen receptor antagonist; meteneprost is a synthetic prostaglandin E analogue; and verapamil is an L-type calcium-channel blocker.
[a]This combination was chosen for experimental validation.

potentially reverse 51 genes, trichostatin A could reverse 70 genes, and the combination of these two drugs could reverse 119 genes under the first threshold criteria (Table 1). In addition, under the more stringent criterion, captopril could reverse 23 genes and vironostat could reverse 37 genes, while their combination could reverse 58 genes (Supplemental Table 3). Among these genes, only a few, such as *CCL2* and *SLC33A1* (under the less stringent criterion) are predicted to be reversed by both drugs, suggesting that these two classes of drugs are probably acting through distinct pathways.

In vivo Validation: Combination Therapy with ACEI and HDACI Provides an Additive Effect Compared with Monotherapy

We used benazepril (an ACEI), which is a drug similar to captopril, and vorinostat (SAHA) as the HDACI to treat Tg26 mice and their age- and sex-matched wild-type littermates. SAHA was chosen instead of trichostatin A because it is an already FDA-approved drug, whereas HDACI is currently used for treating patients with various types of cancer.[16] Benazepril was used in the study because it has a longer half-life than captopril. Tg26 mice usually develop proteinuria at age 4 weeks and progressively proceed to renal failure at age 8–12 weeks. We found that after 6 weeks of therapy, benazepril or SAHA alone reduced proteinuria, improved renal function, and attenuated kidney injury in Tg26 mice compared with mice treated with vehicle (Figures 1 and 2). Moreover, mice treated with both benazepril and SAHA had significantly less proteinuria and kidney injury and better renal function than mice treated with benazepril or SAHA alone, indicating that the combined therapy provided additive renal protective effect compared with the two monotherapies alone (Figures 1 and 2). The kidney histologic features of these mice were scored (Table 2) and were consistent with renal function. We did not observe any abnormal behavior or changes in physical conditions in these mice, regardless of whether the mice were treated with monotherapy or combined therapy. In addition, body weight did not differ between the mice treated with vehicle, monotherapy, or combined therapy (Table 3).

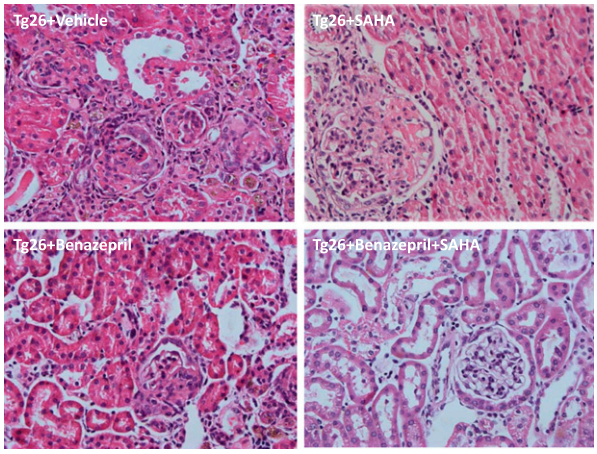

Figure 1. Combination therapy with ACEI and HDACI attenuates kidney injury more significantly than monotherapy. Kidney histology of these mice was analyzed after PAS staining. The representative pictures are shown. Original magnification, x400.

Validation of Gene Expression Changes in Kidney Cortices from Mice Treated with Benazepril or SAHA Alone or in Combination

Next we aimed to determine whether genes predicted to be reversed by these two drugs computationally were indeed reversed in the kidney cortices of mice treated with the drugs. From each group, we selected genes that most likely play a role in the pathogenesis of HIVAN according to previous studies (Table 4) and then measured their expression levels by

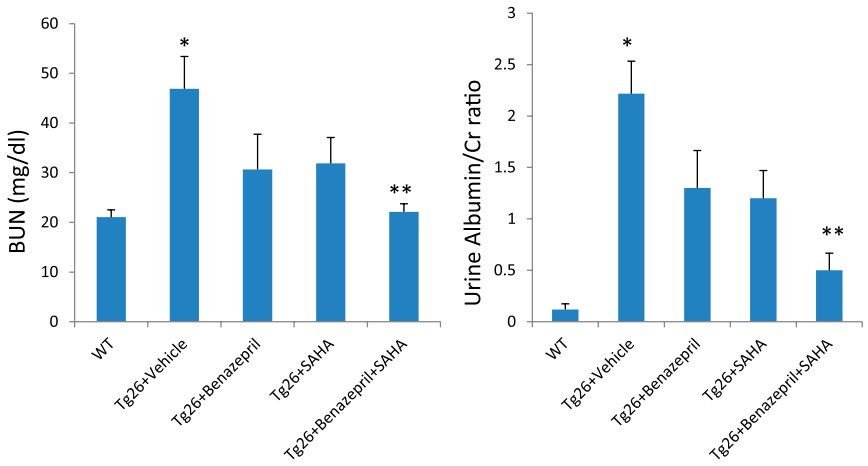

Figure 2. Combination therapy with ACEI and HDACI improves renal function and reduces proteinuria more than monotherapy. At euthanasia, blood and urine samples were collected for determination of BUN and urinary albumin and creatinine (Cr) ratio as described in the Concise Methods section. *$P<0.01$ compared with all other groups, **$P<0.01$ compared with Tg26 mice treated with benazepril or SAHA, $n=6$. Data are means ± SD. Cr, creatinine; WT, wild-type.

Table 2. Summary of kidney histology scoring

Variable	Glomerulosclerosis Index	Podocyte Hypertrophy	Tubular (Casts/Cysts)
WT	0	0	0
Tg26 + vehicle	17.2±6.1	2±0.7	12.6±3.9
Tg26 + benazepril	6.3±2.3[a]	0.7±0.5[a]	5.3±1.6[a]
Tg26 + SAHA	6.0±2.8[a]	0.7±0.8[a]	4.7±2.1[a]
Tg26 + benazepril + SAHA	1.3±1.6[b]	0±0[b]	0.7±1.0[b]

Kidney histologic features of these mice were scored as described in the Concise Methods section after periodic acid-Schiff staining. Values are expressed as mean score ± SD. WT, wild-type.
[a]$P<0.01$ compared with Tg26 + vehicle; $n=6$.
[b]$P<0.05$ compared with Tg26 + benazepril or Tg26 + SAHA; $n=6$.

Table 3. Body weight of mice

Variable	Mean Body Weight ± SD Before Treatment (g)	Mean Body Weight ± SD At Euthanasia (g)
WT	20.25±2.30	22.35±3.02
Tg26 + vehicle	17.72±2.72	19.32±2.19
Tg26 + benazepril	18.97±2.43	21.37±2.27
Tg26 + SAHA	17.68±1.79	20.02±2.93
Tg26 + benazepril + SAHA	19.28±2.30	21.75±2.29

Body weight was recorded for these mice before the treatment and at the end of the experiment. No significant difference was observed among the groups ($n=6$).

real-time PCR. We found that eight out of the nine selected genes were reversed in the kidneys of these mice by benazepril treatment, and 9 of 11 selected genes were reversed by SAHA treatment (Figure 3, A and B). The two overlapping genes (*CCCL2* and *SLC7A1*) that were predicted to be regulated by both benazepril and SAHA were indeed inhibited in kidneys of Tg26 mice treated with benazepril or SAHA (Figure 3, A and B).

Pathway Analysis of Genes Altered in Tg26 Kidneys and Predicted to be Reversed by ACEI and HDACI

To understand the molecular mechanisms behind how these two drugs work alone or together, we performed pathway enrichment analysis on the genes predicted to be reversed by these two drugs. We applied gene list enrichment analysis using the BioCarta, KEGG (Kyoto Encyclopedia of Genes and Genomes [KEGG]),[17] WikiPathways,[18] ChIP-seq/chip enrichment analysis (ChEA),[19] kinase enrichment analysis (KEA),[20] protein interaction hubs, Mouse Genome Informatics-Mammalian Phenotype,[21] and Human Gene Atlas (cell types expression)[22] gene set libraries implemented within our software tools Lists2Networks[23] and Expression2Kinases[24] (Supplemental Tables 4–7). These tools use the Fisher exact test to compute *P* values for probability for overlap between two independent sets of genes. To visualize the results, we created square grids in which each square represents a gene set library term (*e.g.*, a specific cell signaling pathway from BioCarta, WikiPathways, or KEGG) (Figure 4, A–D). Bright squares represent enriched overlapping terms *P* values, and terms are organized on the grid based on their gene content similarity.

The enriched terms are affected by drug treatments based on overlapping genes associated with the term and also affected by the treatments with captopril or trichostatin A. Some top overlapping terms/squares are annotated, and the complete enrichment analysis results are provided in Supplemental Tables 4–7.

The enrichment analysis for the differentially expressed genes in Tg26 mice that are predicted to be reversed by trichostatin A show enrichment for genes that are highly expressed in immune cells, such as CD14+ monocytes, CD33+ myeloid, and BDCA4+ dendritic cells based on the Human Gene Atlas gene set library. This gene set library was created by identifying genes that are highly expressed in a specific tissue compared with the average and SD expression of the gene in 84 different human cell types.[22] Abnormal immune system was also reported based on the Mouse Genome Informatics-Mammalian Phenotype gene set library enrichment analysis. This library is created from the Mouse Phenotype ontology developed by the Jackson Lab, where knockout genes in mice are assigned to mouse phenotype ontology;[21] Toll-like receptor and NFκB pathways are enriched on the basis of BioCarta pathways; the GATA1 transcription is enriched according to ChEA[19]; and Erk1 and PI3K are enriched protein hubs. The protein hub library includes all proteins with 50 or more known direct binding partners; the IRAK1 kinase substrates are enriched based on KEA;[20] and IL-3, IL-5, and IL-6

Table 4. Overlapping genes of drugs and differentially expressed genes in HIVAN kidneys for trichostatin A and captopril from Table 1

Drug and Direction	Gene
Trichostatin A overlapping genes predicted to be restored in desired direction	−*CSF2RA*, +*ALDH6A1*, −*MBP*, −*TNFRSF1A*, −*MYC1*, −*WIPF1*, −*IFIT1*, −*C3AR1*, −*ZFP36L2*, −*LMNA*, −*CCNA2*, −*DGCR8*, −*IL16*, −*NFKB1*, −*ATF5*, −*PPP2R1A*, −*SLC7A1*, +*SRR*, −*RCN1*, +*SCRN3*, +*TPMT*, −*SOX4*, +*PRKACA*, −*SLA*, −*CREM*, −*FGL2*, −*TRPV2*, −*PLEKHO1*, −*LAIR1*, +*ACO1*, +*TRIM23*, −*LRRK1*, −*RGS19*, +*MYO6*, −*HCK*, −*PON2*, −*FES*, −*CLCF1*, −*MYD88*, +*ALDH8A1*, −*CD84*, −*DDX58*, −*PTPRS*, +*HOXA7*, +*PEX1*, −*ITGAL*, −*GLIPR1*, −*INPP5D*, −*CCL2*, −*P2RY6*
Trichostatin A overlapping genes exacerbated in undesired direction	+*ABCG1*, +*ANKRD6*, +*ATP13A2*, +*ATP6V1C1*, +*BIRC3*, +*CRISPLD2*, +*DAAM1*, +*DSE*, +*GCH1*, +*GRK5*, +*GUCY1B3*, +*KDELC1*, +*MARCKS*, +*PICALM*, +*PITPNA*, +*RRAS*, +*SERPINB9*, +*TMEM45A*, −*TOR1A*, −*VLDLR*, −*METTL8*, −*LASS2*
Captopril overlapping genes predicted to be restored in desired direction	−*ADRBK1*, −*CCDC88A*, +*PARP16*, −*MOBKL1B*, −*MAPKAPK3*, +*PSMC3IP*, −*PLP2*, −*AP1S2*, −*MAN1C1*, −*CD44*, −*FXYD5*, −*MBNL1*, −*SKAP2*, −*RHOG*, −*PTPRC*, −*CXCR4*, −*S100A11*, −*TPM4*, −*ENSA*, −*HIP1*, −*LAPTM5*, +*HIBCH*, −*ALDH18A*, −*SLC7A1*, +*ZFAND1*, +*CRADD*, −*TAP2*, −*CHMP2B*, +*MTFR1*, −*IFNGR1*, −*GNB2*, −*RAC2*, −*NONO*, −*BICD2*, −*LCP1*, −*STAT3*, −*CD99*, +*SLC33A1*, −*CASP1*, +*RWDD3*, −*CCL2*, −*MAPRE1*, −*SH3BGRL3*, −*SMC3*, −*TAGLN2*, −*CALU*, −*PLEK*, +*SAC3D1*, −*PICALM*, +*RHBDD3*, −*PSAT1*
Captopril overlapping genes exacerbated in undesired direction	+*AP1S2*, +*ATF5*, +*ATP8B2*, +*B4GALNT1*, +*BRD4*, +*CD93*, +*CR1*, +*DBN1*, +*DGCR8*, +*DPY19L1*, +*ENC1*, +*GPNMB*, +*GRK5*, +*HIVEP3*, +*LMNA*, +*MCL1*, +*MMP2*, +*PCDHGA1*, +*PON2*, +*PTGER4*, +*RCN1*, +*RPS11*, +*TAPBP*, +*TBC1D2B*, −*SLC25A40*, −*ZKSCAN1*, −*NXT2*, −*USP34*, −*TOR1A*, −*CAT*, −*LYRM2*

Trichostatin A and captopril could reverse the maximal number of genes (n=119) altered in Tg26 kidneys while exacerbating a minimal number of genes (n=51). Among these genes, many are known to be critically involved in HIVAN, such as *CCL2*, *NFκB1*, *CCNA2*, and *MYC*. Two genes (*CCL2* and *SLC7A1*) are overlapped between trichostatin A and captopril. The highlighted genes (red) were selected because they are known to be involved in the kidney disease and were further tested experimentally. These genes were validated by real-time PCR, as shown in Figure 3. − indicates decrease; + indicates increase.

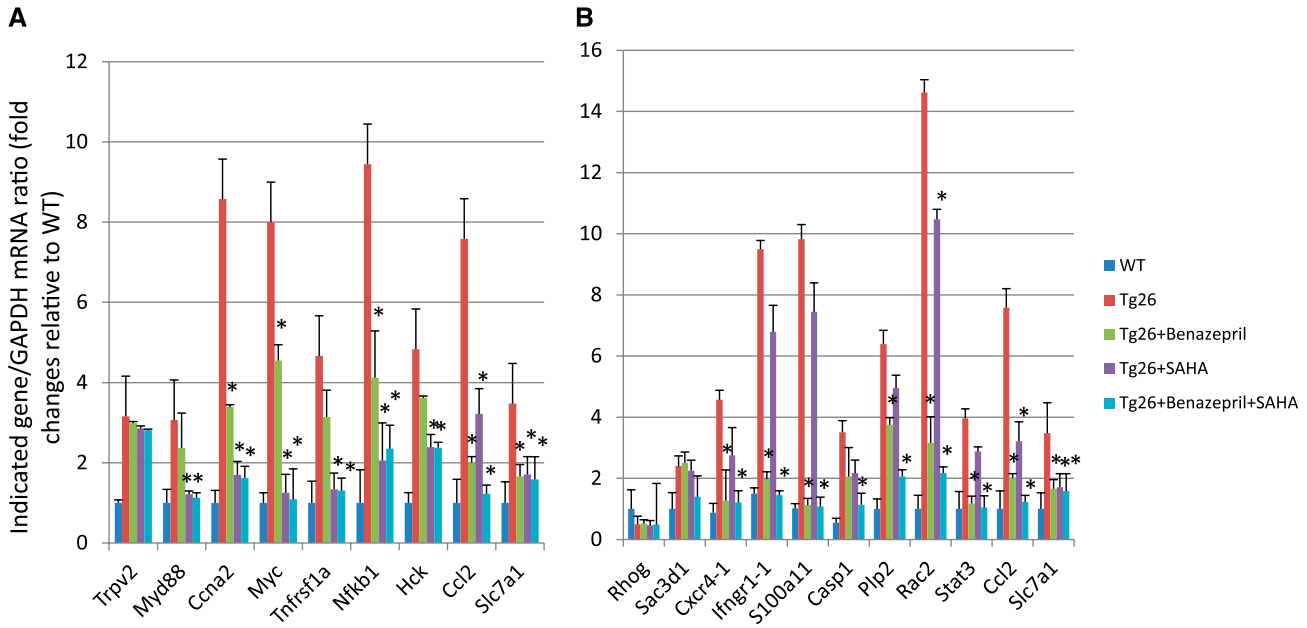

Figure 3. Validation of expression of genes that are altered in Tg26 kidneys and predicted to be reversed by ACEI or HDACI. Total RNA was isolated from kidney cortices of Tg26 mice treated with vehicle, SAHA, or benazepril. Real-time PCR was analyzed for the genes that are altered in Tg26 kidneys and predicted to be reversed by HDACI (A) or reversed by ACEI (B) or both (C). Data are means ± SD. n=6; *P<0.01 compared with Tg26 mice treated with vehicle. GAPDH, glyceraldehyde 3-phosphate dehydrogenase; WT, wild-type.

pathways are based on WikiPathways[18] (Figure 4A and Supplemental Table 4). Hence, trichostatin A is an anti-inflammatory drug that reduces inflammation in the kidneys of HIVAN mice, where it is probably acting through the IL and NFκB pathways. We also analyzed the enriched terms for all (n=1000) up and down differentially expressed genes affected

by trichostatin A treatment for the particular experiment in CMAP that maximally reversed genes from our HIVAN model (experiment 6193 in CMAP). The results between CMAP alone versus CMAP + Tg26 are not surprisingly similar because the input lists for Figure 4, A and B share a sizable number of genes. However, there is a difference because one list is directly from CMAP and the other is the subset that overlaps with the gene differentially expressed in Tg26. Although we are comparing drug effects on human cancer cells to disease effects on mouse kidney tissue, we hope that the affected genes by the drug in human cells are preserved somewhat in the mouse tissue. Of note, the highest enriched term from the BioCarta gene set library analysis, for all the differentially expressed genes from experiment 6193 in CMAP before consideration of the overlap with Tg26, is the HIV-Nef pathway. Other enriched terms are the NFκB pathway (Bioarta) and apoptosis pathways (WikiPathways and BioCarta) (Figure 4B and Supplemental Table 5).

Interestingly, and although for a completely different set of input genes, the enrichment analysis for the differentially expressed genes in Tg26 mice that are potentially reversed by captopril, also show enrichment for genes that are highly expressed in immune cells such as CD14+ monocytes, CD33+ myeloid, BDCA4+ dendritic cells based on the Human Gene Atlas, and abnormal immune system based on Mouse Genome Informatics-Mammalian Phenotype. However, this effect is mediated through different pathways: SMAD1 and SMAD2 are the enriched transcription factors based on the ChEA gene set library; IL7R, TGFBR1, CASP8, JAK1, JAK2 are the enriched protein hubs; JAK1–3 and TGFBR1 have many kinase substrates based on the KEA gene set library; and apoptosis, IL-3, IL-7, IL-9 and TGF-β pathways based on WikiPathways (Figure 4C and Supplemental Table 6). We also analyzed the enriched terms for all (n=1000) the up and down differentially expressed genes affected by captopril treatment for the particular experiment in CMAP that maximally reversed genes from our HIVAN model (experiment 1988 in CMAP). As was seen with the same analysis for trichostatin A, the results for all the differentially expressed genes from experiment 1988 in CMAP before consideration of the overlap with Tg26 are consistent with the enrichment shown in Figure 4C. The overlapping genes show enrichment for the p38, apoptosis, and oxidative stress pathways (Figure 4D and Supplemental Table 7); p38 also stands out with many substrates based on the KEA analysis. Hence, both drugs appear to be anti-inflammatory but working through different pathways: trichostatin A through NFκB signaling and captopril through TGF-β/Smad, Jak/Stat3, and

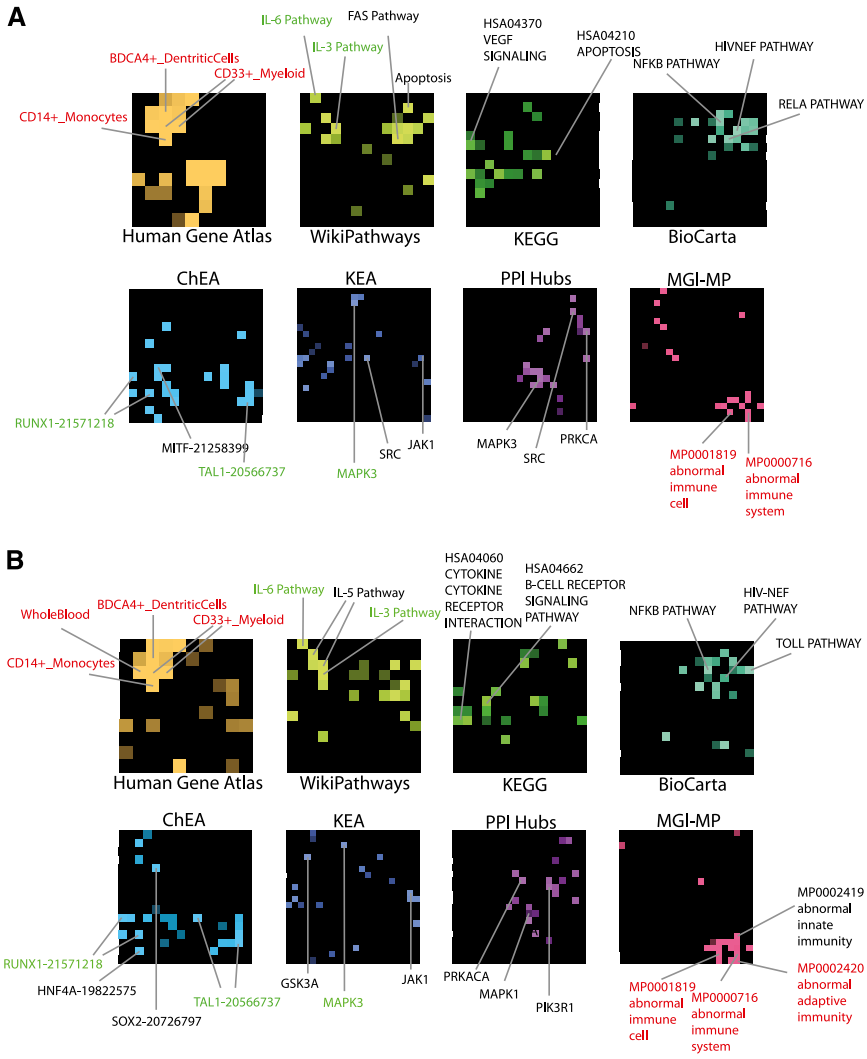

Figure 4. Pathway analysis of gene lists affected by trichostatin A and captopril shows highly enriched pro-inflammatory and pro-fibrosis pathways. Eight different gene set libraries are visualized as square grids in which each library term is represented by a square. Squares are organized on the grid by their gene content similarity using simulated annealing. Bright squares represent high overlapping genes with the query list. Top enriched terms computed using the Fisher exact test are highlighted in brighter colors based on *P* value. Some top overlapping terms/squares are annotated; some terms are colored to distinguish terms that appear to be enriched for all input lists (red) and those consistent for CMAP only and CMAP+Tg26 (green and turquoise). For each input list, (A) trichostatin A (CMAP overlap with Tg26), (B) trichostatin A (CMAP only), (C) captopril (CMAP overlap with Tg26), and (D) captopril (CMAP only) are represented by eight different grids. The full enrichment results are available in Supplemental Tables 4–7. MGI-MP, Mouse Genome Informatics-Mammalian Phenotype; PPI Hubs, protein-protein interaction hubs.

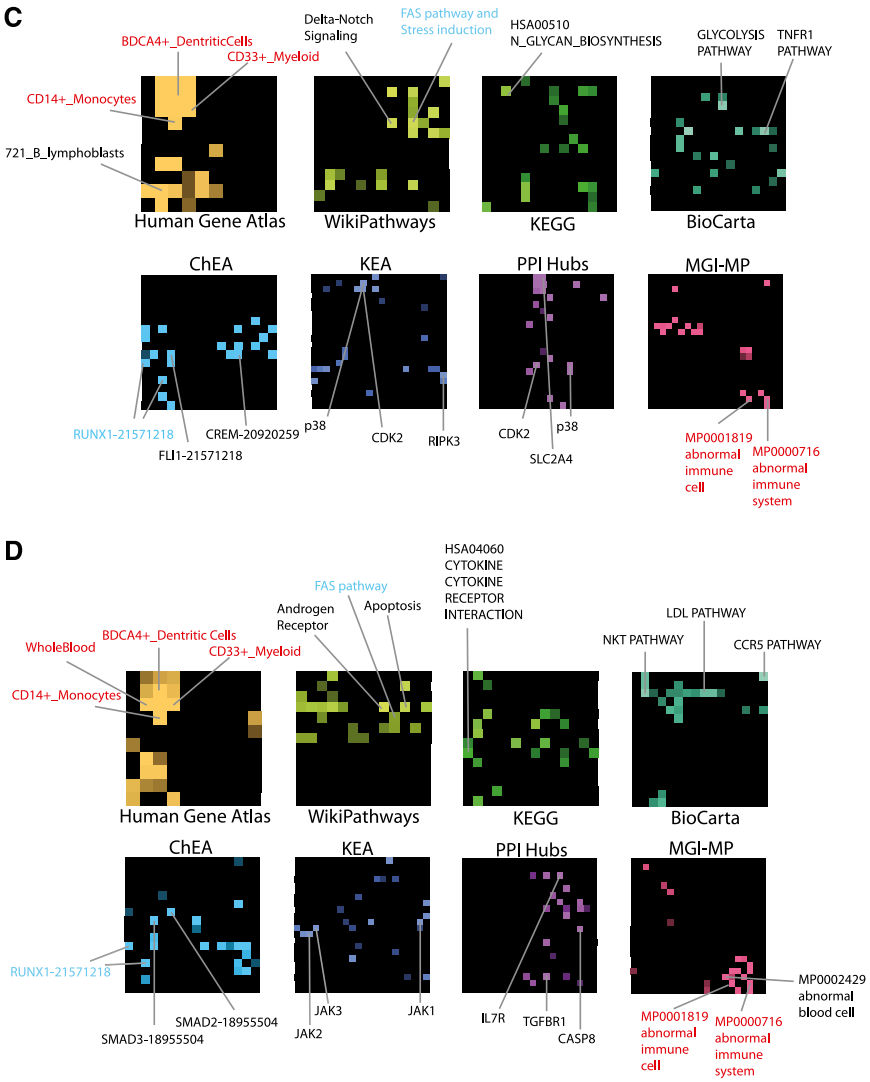

Figure 4. Continued.

p38/oxidative stress pathways. All these pathways are well known to be involved in the pathogenesis of HIVAN as well as in other kidney fibrotic diseases.

Pathway Validation in Kidneys of Mice Treated with Benazepril or SAHA Alone or in Combination

Because the pathway analysis shows that NFκB-mediated inflammatory pathway is more specific for trichostatin A and that TGF-β/Smad, p38/oxidative stress pathways are more specific for captopril, we selected these pathways for further experimental validation. These pathways are already known to be involved in HIVAN as well as in other kidney diseases. [25–28] We confirmed that SAHA affects more NFκB target genes in kidneys of Tg26 mice than does benazepril, whereas benazepril affects more Smad3 and p38 phosphorylation and oxidative stress (as measured by reduced glutathione and oxidized glutathione ratio) than SAHA (Figure 5). It is known that activation of the angiotensin system induces Smad3 phosphorylation and oxidative stress[29–31] whereas HDAC interacts with the NFκB pathway.[32] Our findings are consistent with our computational predictions. These results support that SAHA and benazepril probably affect distinct pathways in the diseased kidney.

DISCUSSION

A large body of evidence suggests that ACEI or ARBs slow the progression of kidney disease. However, these drugs do not completely stop disease progression. Therefore, it is critical to develop more effective therapies. Here, we developed a general approach to predict the potential of drug combinations to reverse the abnormal gene expression observed in HIVAN. Our analysis identified the combination of ACEI and HDACI as potentially having the most effective outcome for drug pairs among the approximately 1300 drugs and 6000 experiments computationally screened to reverse the abnormal gene expression observed in HIVAN. ACEIs are already known to provide renal protection and have been used clinically to treat patients with kidney disease.[14] However, ACEIs and HDACIs together have never been tested. Our analysis predicts that the combination of ACEI and HDACI could reverse 119 genes, which make up about 25% of the genes significantly altered in the diseased kidney from a mouse model of HIVAN. The combination therapy is probably affecting several important pathways involved in kidney inflammation and fibrosis, including NFκB, IL, TGF-β, mitogen-activated protein kinase, and apoptosis signaling. Both drugs are probably anti-inflammatory but work through different pathways with a converged phenotype.

Our approach has several limitations. The fact that the data in CMAP were obtained from human cancer cell lines makes these data of questionable relevance to kidney cells and kidney disease in mice. Our approach is based on the assumption that even though CMAP was created using human cancer cell lines, the direction of gene expression induced by drugs is preserved across cell types and organisms. This assumption has not been proven yet and could be true only for some drugs and some cell types. However, our results from the computational analysis and the validation experiments are consistent with this hypothesis. Future studies are required to validate this approach more globally. Ideally, we would test many combinations

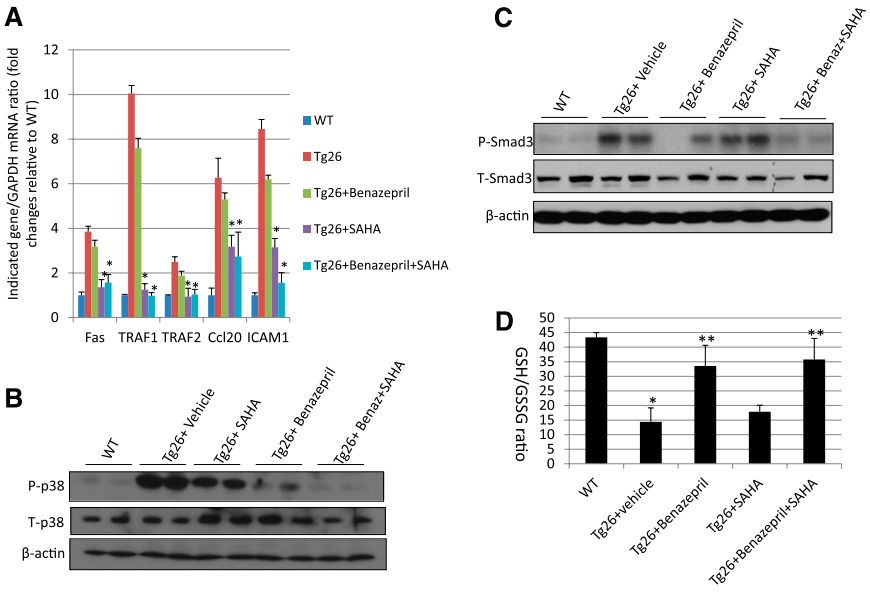

Figure 5. Validation of the pathways predicted to be affected by ACEI or HDACI. (A) Real-time PCR analysis of NFκB target genes in kidneys of Tg26 mice treated with SAHA or benazepril or both. $n=6$; *$P<0.01$ compared with Tg26 mice treated with vehicle. (B and C) Western blotting analysis of phosphor-p38, total-p38, phosphor-Smad3, total-Smad3, and β-actin. The representative blots are shown. (D) Reduced glutathione and oxidized glutathione were measured by the kit as described and the ratio was calculated. $n=6$; *$P<0.01$ compared with wild-type, **$P<0.01$ compared with Tg26 mice treated with benazepril. GAPDH, glyceraldehyde 3-phosphate dehydrogenase; GSH/GSSG, reduced glutathione and oxidized glutathione; WT, wild-type. Data are means ± SD.

of drugs to assess the quality of the rankings that the computational method produced. Testing many drug combinations in mice is expensive and time consuming, and thus is not feasible. Therefore, we selected the most promising pair (ACEI plus HDACI) for further testing on the basis of the existing evidence suggesting that these drugs may work in combination. ACEI is considered as the current standard therapy to treat kidney disease,[14] and our combination therapy was compared with ACEI monotherapy, which is consistent with all current clinical trials for kidney disease. One advantage of using CMAP is that it includes most FDA-approved drugs. Thus, drugs combinations identified from CMAP could be quickly translated to clinical trials for repositioning and repurposing. In addition, our findings support that the drug predictions from CMAP have potential implication for other forms of kidney disease besides HIVAN, and perhaps nonkidney fibrotic diseases, such as liver fibrosis.

Although the incidence of HIVAN has decreased because of antiretroviral therapy, the disease prevalence remains high as a result of aging of the cohort.[33,34] Kidney disease in these patients is probably related to diseases of accelerated aging, including arteriosclerosis, hypertension, and diabetes. Tg26 mouse is an excellent animal model for CKD because it recapitulates many of the findings seen in humans, including glomerulosclerosis and interstitial fibrosis.[35,36] Because ACEI is known to have renal protection in many kinds of kidney diseases and HDACI is known to have general antifibrosis effects, it is likely that combination therapy with these two drugs could provide renal protection in many forms of kidney disease.

Our study suggests that a clinical trial combining ACEI and HDACI might be warranted. The adverse effects of ACEI are well documented, including hyperkalemia and worsening of renal function. These adverse effects are unlikely to be enhanced by HDACI. In addition, our prediction attempted to exclude the drug combinations that could exacerbate the expression of genes already altered in the diseased kidney. We hope that this part of the strategy could help to avoid some potential adverse effects caused by combination therapy. We did not observe any obvious adverse effects in our animal studies. However, this does not mean that combination therapy with ACEI and HDACI will not cause serious adverse effects in humans. Future studies are required to confirm the effects of this combination therapy in other animal models and for longer duration of therapy before this approach can be applied in humans. In addition, it will be interesting to further determine the mechanisms of the interaction between ACEI and HDACI. A limitation of the study is that the effect of these inhibitors on BP was not assessed in these animals. It has been reported that Tg26 displays slightly elevated BP compared with wild-type littermates and that ARBs can reduce BP in Tg26 mice.[37,38]

In summary, we used a computational approach to predict a drug combination based on a database of drug-induced gene expression signatures. This tool helped us to predict potential drug combinations after incorporating the differential gene expression profiles from the disease model of HIVAN. Using this approach, we predicted that the combination of ACEI and HDACI provides additive effects in improving the status of kidney injury in the Tg26 mouse. Then, we experimentally validated this combination therapy to show that it does indeed provide additive renal protection compared with monotherapy. We also analyzed and experimentally validated the potential pathways mediating the protective effects of these drugs. Our approach can be used for searching drug combinations for kidney diseases and other disorders. Users are provided with an easy-to use software tool called DPS to test the approach in other contexts.

CONCISE METHODS

Prioritizing Pairs of Drugs

From the CMAP database at http://www.broadinstitute.org/cmap/, we first downloaded the ranked lists of probes table. This table is freely available for download and provides the ranks of all genes as

microarray probes based on their change in expression after all the approximately 6000 drug perturbation experiments. From this table, we extracted the top and bottom 500 differentially expressed genes by converting probe identification numbers to Entrez gene symbols using the Affymetrix lookup table associated with the platform. Probe identification numbers for the same genes were condensed to the most high or low expressed probes. To compute pairwise combinations of drugs for sets of up and down differentially expressed gene lists, we assume some degree of additivity within the perturbing effects of pairs of drugs (*i.e.*, the perturbation resulting from drug d_i and drug d_j acting in combination is $d_i + d_j$, then given as input a set of up- and downregulated genes determined between two conditions), and using the top 500 and bottom 500 genes affected by all the drug perturbation experiments from CMAP, we identify pairs of drugs that maximally flip the expression of the inputted differentially expressed genes and minimally exacerbate the expression of the input genes as follows:

$$\begin{aligned}&\textit{Score for reversing expression back to the control state}\\&= \left[(up \cap down_{di}) + \left(up \cap down_{dj}\right) + (down \cap up_{di})\right.\\&\quad \left. + (down \cap up_{di})\right] - \left[(up \cap up_{di}) + \left(up \cap up_{dj}\right)\right.\\&\quad \left. + (down \cap downd_{di}) + \left(down \cap downd_{dj}\right)\right]\end{aligned}$$

Where ∩ means intersection between two sets; up- indicates a lists of upregulated genes in disease; down- indicates a list of downregulated genes in disease; up_{di} indicates genes upregulated by a drug in the *i*th experiment in CMAP; and $down_{di}$- indicates genes downregulated by a drug in the *i*th experiment in CMAP. No proportion test or normalization is needed because all the lists from CMAP are of the same size. Because searching for all combinations is computationally expensive, we devised a simple heuristic that performs optimally without covering the entire search space. We first search for all single drugs that have a maximal score as described above. Then, for the top 100 ranked drugs from the initial single drug search, we search the second drug that in combination with the first drug would have the maximal score. A software tool that allows users to perform the same analysis for any sets of differentially expressed genes, and a dedicated website for hosting the software online with a user manual is provided at http://www.maayanlab.net/DPS.

Animal Studies

Male Tg26 mice at age 4 weeks were given vehicle, SAHA at 50 mg/kg per day (Cayman Chemical Company, catalog no. 10009929), benazepril at 10 mg/kg per day (Sigma, catalog number B0935), or SAHA plus benazepril by daily gavage (n=6) for 6 weeks. The vehicle was made by an aqueous 4% methyl solution (Sigma M0262) containing 1.3% polyethylene glycol (Fluka 81172). Body weights were recorded before the treatment and at the end of the treatment. Unrestricted food and water were provided throughout the duration of the experiment. So that blood, urine, and tissue could be collected, the mice were euthanized at 10 weeks of age by exposure to carbon monoxide. All animal studies were performed according to the protocols approved by Institutional Animal Care and Use Committee at the Mount Sinai School of Medicine.

Measurement of BUN, Urine Protein, and Creatinine

BUN was measured by using a commercially available kit (Bioassay Systems, Hayward, CA). Urine albumin was quantified by ELISA using a kit from Bethyl Laboratory Inc. (Houston, TX). Urine creatinine levels were measured in the same samples using QuantiChrom Creatinine Assay Kit (DICT-500) (BioAssay Systems) according to the manufacturer instruction. The urine albumin excretion rate was expressed as the ratio of albumin to creatinine.

Quantitative Histopathology

Mice were perfused with PBS containing 4% paraformaldehyde, and kidneys were further fixed in 4% paraformaldehyde for 2 hours. Kidney tissue was embedded into paraffin. Kidney histologic features were examined after periodic acid-Schiff staining. Glomerulosclerosis was scored as described previously by Dr. D'Agati.[39] Briefly, each specimen received a score for three measures: percentage of glomerulosclerosis, percentage of tubular cysts or casts, and podocyte hypertrophy. The percentage of glomerulosclerosis was obtained by identifying the total number of glomeruli with any sclerosis and dividing this number by the total number of glomeruli seen. The percentage of tubular cysts or casts score was obtained by the number of tubules with microcystic dilatation or tubules filled with casts divided by the total number of tubular cross sections in a representative area. Finally, the degree of podocyte hypertrophy was scored as 0 (absence), 1+ (podocyte hypertrophy observed in <25% of all glomeruli), 2+ (podocyte hypertrophy observed in 25%–50% of all glomeruli), and 3+ (podocyte hypertrophy in >50% of all glomeruli).

Real-time PCR

Total RNA was isolated from kidney cortices of these mice using TRIzol (Invitrogen). Real-time PCR was performed with a Roche Lightcycler and Qiagen QuantiTect One Step RTPCR SYBR green kit (Qiagen) according to the manufacturer's instructions. Predesigned primer sets were obtained from Qiagen (GeneGlobe), and the sequences are listed in Supplemental Table 8. Light cycler analysis software was used to determine crossing points using the second derivative method. Data were normalized to housekeeping genes (tubulin) and presented as fold increase compared with RNA isolated from wild-type animals using the $2^{-\Delta\Delta CT}$ method.

Western Blot

Kidney cortices were lysed with a buffer containing 1% Triton, a protease inhibitor cocktail, and tyrosine and serine-threonine phosphorylation inhibitors. Lysates were subjected to immunoblot analysis using antibodies for phosphor- and total p38, Smad3 (Cell Signaling), and anti–glyceraldehyde 3-phosphate dehydrogenase (Sigma).

Measurement of Reduced Glutathione and Oxidized Glutathione Ratio

Reduced glutathione and oxidized glutathione were analyzed in tissue lysates of kidney cortices with a colorimetric reaction kit (OxisResearch, Portland, OR) using a modified protocol based on the manufacturer's instructions. The levels were first normalized to the protein concentration of kidney tissue lysates and the ratio was determined.

Statistical Analyses

Data are expressed as mean ± SD. The unpaired Bonferroni corrected *t* test was used to identify differentially expressed genes between two groups. Statistical significance was considered at the $P<0.05$ threshold. The statistics used for the other computational analyses are described in the text.

ACKNOWLEDGMENTS

Y.Z. is supported by the National Natural Science Foundation of China for Young Investigators (1999-30901944), J.C.H. is supported by National Institutes of Health (NIH) grants 1R01DK088541 and 1R01DK078897, Chinese 973 fund 2012CB517601, and Veterans Affairs Merit Award 2I01BX000345-04. A.M. is supported by NIH grants R01GM098316, U54HG006097-02S1, P50GM071558, and R01DK088541. J.C.H., A.M., and P.E.K. are supported by NIH grants P01-DK-56492 and 1RC4DK090860. P.Y.C. is supported by NIH grant 5K08DK082760.

DISCLOSURES

None.

REFERENCES

1. Maione A, Navaneethan SD, Graziano G, Mitchell R, Johnson D, Mann JF, Gao P, Craig JC, Tognoni G, Perkovic V, Nicolucci A, De Cosmo S, Sasso A, Lamacchia O, Cignarelli M, Manfreda VM, Gentile G, Strippoli GF: Angiotensin-converting enzyme inhibitors, angiotensin receptor blockers and combined therapy in patients with micro- and macroalbuminuria and other cardiovascular risk factors: A systematic review of randomized controlled trials. *Nephrol Dial Transplant* 26: 2827–2847, 2011
2. Persson F, Rossing P, Schjoedt KJ, Juhl T, Tarnow L, Stehouwer CD, Schalkwijk C, Boomsma F, Frandsen E, Parving HH: Time course of the antiproteinuric and antihypertensive effects of direct renin inhibition in type 2 diabetes. *Kidney Int* 73: 1419–1425, 2008
3. Bomback AS, Kshirsagar AV, Amamoo MA, Klemmer PJ: Change in proteinuria after adding aldosterone blockers to ACE inhibitors or angiotensin receptor blockers in CKD: A systematic review. *Am J Kidney Dis* 51: 199–211, 2008
4. Navaneethan SD, Nigwekar SU, Sehgal AR, Strippoli GF: Aldosterone antagonists for preventing the progression of chronic kidney disease: A systematic review and meta-analysis. *Clin J Am Soc Nephrol* 4: 542–551, 2009
5. Azizi M, Menard J: Renin Inhibitors and Cardiovascular and Renal Protection: An Endless Quest? [published online ahead of print March 6, 2012] *Cardiovasc Drugs Ther* doi:10.1007/s10557-012-6380-6
6. Kunz R, Friedrich C, Wolbers M, Mann JF: Meta-analysis: Effect of monotherapy and combination therapy with inhibitors of the renin angiotensin system on proteinuria in renal disease. *Ann Intern Med* 148: 30–48, 2008
7. Mancia G: Angiotensin receptor antagonists and increased risk of cancer. Further evidence against. *J Hypertens* 29: 653–654, 2011
8. Slagman MC, Navis G, Laverman GD: Dual blockade of the renin-angiotensin-aldosterone system in cardiac and renal disease. *Curr Opin Nephrol Hypertens* 19: 140–152, 2010
9. Redon J, Mancia G, Sleight P, Schumacher H, Gao P, Pogue J, Fagard R, Verdecchia P, Weber M, Böhm M, Williams B, Yusoff K, Teo K, Yusuf S; ONTARGET Investigators: Safety and efficacy of low blood pressures among patients with diabetes: Subgroup analyses from the ONTARGET (ONgoing Telmisartan Alone and in combination with Ramipril Global Endpoint Trial). *J Am Coll Cardiol* 59: 74–83, 2012
10. Dannenfelser R, Xu H, Raimond C, Ma'ayan A: Network pharmacology to aid the drug discovery process. In: *New Frontiers of Network Analysis in Systems Biology*, edited by Macarthur AMAAB, Dordrecht, the Netherlands, Springer Science, 2012
11. Lamb J, Crawford ED, Peck D, Modell JW, Blat IC, Wrobel MJ, Lerner J, Brunet JP, Subramanian A, Ross KN, Reich M, Hieronymus H, Wei G, Armstrong SA, Haggarty SJ, Clemons PA, Wei R, Carr SA, Lander ES, Golub TR: The Connectivity Map: Using gene-expression signatures to connect small molecules, genes, and disease. *Science* 313: 1929–1935, 2006
12. Iorio F, Rittman T, Ge H, Menden M, Saez-Rodriguez J: Transcriptional data: A new gateway to drug repositioning? [published online ahead of print August 7, 2012] *Drug Discov Today* doi: 10.1016/j.drudis.2012.07.014
13. Jin Y, Ratnam K, Chuang PY, Fan Y, Zhong Y, Dai Y, Mazloom AR, Chen EY, D'Agati V, Xiong H, Ross MJ, Chen N, Ma'ayan A, He JC: A systems approach identifies HIPK2 as a key regulator of kidney fibrosis. *Nat Med* 18: 580–588, 2012
14. Lewis EJ, Hunsicker LG, Bain RP, Rohde RD; The Collaborative Study Group: The effect of angiotensin-converting-enzyme inhibition on diabetic nephropathy. *N Engl J Med* 329: 1456–1462, 1993
15. Pang M, Kothapally J, Mao H, Tolbert E, Ponnusamy M, Chin YE, Zhuang S: Inhibition of histone deacetylase activity attenuates renal fibroblast activation and interstitial fibrosis in obstructive nephropathy. *Am J Physiol Renal Physiol* 297: F996–F1005, 2009
16. Butler LM, Zhou X, Xu WS, Scher HI, Rifkind RA, Marks PA, Richon VM: The histone deacetylase inhibitor SAHA arrests cancer cell growth, upregulates thioredoxin-binding protein-2, and down-regulates thioredoxin. *Proc Natl Acad Sci U S A* 99: 11700–11705, 2002
17. Ogata H, Goto S, Fujibuchi W, Kanehisa M: Computation with the KEGG pathway database. *Biosystems* 47: 119–128, 1998
18. Kelder T, van Iersel MP, Hanspers K, Kutmon M, Conklin BR, Evelo CT, Pico AR: WikiPathways: building research communities on biological pathways. *Nucleic Acids Res* 40[Database issue]: D1301–D1307, 2012
19. Lachmann A, Xu H, Krishnan J, Berger SI, Mazloom AR, Ma'ayan A: ChEA: transcription factor regulation inferred from integrating genome-wide ChIP-X experiments. *Bioinformatics* 26: 2438–2444, 2010
20. Lachmann A, Ma'ayan A: KEA: kinase enrichment analysis. *Bioinformatics* 25: 684–686, 2009
21. Blake JA, Bult CJ, Eppig JT, Kadin JA, Richardson JE; Mouse Genome Database Group: The Mouse Genome Database genotypes:phenotypes. *Nucleic Acids Res* 37[Database issue]: D712–D719, 2009
22. Su AI, Wiltshire T, Batalov S, Lapp H, Ching KA, Block D, Zhang J, Soden R, Hayakawa M, Kreiman G, Cooke MP, Walker JR, Hogenesch JB: A gene atlas of the mouse and human protein-encoding transcriptomes. *Proc Natl Acad Sci U S A* 101: 6062–6067, 2004
23. Lachmann A, Ma'ayan A: Lists2Networks: integrated analysis of gene/protein lists. *BMC Bioinformatics* 11: 87, 2010
24. Chen EY, Xu H, Gordonov S, Lim MP, Perkins MH, Ma'ayan A: Expression2Kinases: mRNA profiling linked to multiple upstream regulatory layers. *Bioinformatics* 28: 105–111, 2012
25. Heyman SN, Rosenberger C, Rosen S: Acute kidney injury: Lessons from experimental models. *Contrib Nephrol* 169: 286–296, 2011
26. Ma FY, Liu J, Kitching AR, Manthey CL, Nikolic-Paterson DJ: Targeting renal macrophage accumulation via c-fms kinase reduces tubular apoptosis but fails to modify progressive fibrosis in the obstructed rat kidney. *Am J Physiol Renal Physiol* 296: F177–F185, 2009
27. Ross MJ, Fan C, Ross MD, Chu TH, Shi Y, Kaufman L, Zhang W, Klotman ME, Klotman PE: HIV-1 infection initiates an inflammatory cascade in human renal tubular epithelial cells. *J Acquir Immune Defic Syndr* 42: 1–11, 2006

28. Schmid H, Boucherot A, Yasuda Y, Henger A, Brunner B, Eichinger F, Nitsche A, Kiss E, Bleich M, Gröne HJ, Nelson PJ, Schlöndorff D, Cohen CD, Kretzler M; European Renal cDNA Bank (ERCB) Consortium: Modular activation of nuclear factor-kappaB transcriptional programs in human diabetic nephropathy. *Diabetes* 55: 2993–3003, 2006
29. Liu Z, Huang XR, Lan HY: Smad3 mediates ANG II-induced hypertensive kidney disease in mice. *Am J Physiol Renal Physiol* 302: F986–F997, 2012
30. Palm F, Nordquist L: Renal oxidative stress, oxygenation, and hypertension. *Am J Physiol Regul Integr Comp Physiol* 301: R1229–R1241, 2011
31. Wolf G: Renal injury due to renin-angiotensin-aldosterone system activation of the transforming growth factor-beta pathway. *Kidney Int* 70: 1914–1919, 2006
32. Chen Y, Wang H, Yoon SO, Xu X, Hottiger MO, Svaren J, Nave KA, Kim HA, Olson EN, Lu QR: HDAC-mediated deacetylation of NF-κB is critical for Schwann cell myelination. *Nat Neurosci* 14: 437–441, 2011
33. Lucas GM, Mehta SH, Atta MG, Kirk GD, Galai N, Vlahov D, Moore RD: End-stage renal disease and chronic kidney disease in a cohort of African-American HIV-infected and at-risk HIV-seronegative participants followed between 1988 and 2004. *AIDS* 21: 2435–2443, 2007
34. Wyatt CM, Klotman PE: HIV-associated nephropathy in the era of antiretroviral therapy. *Am J Med* 120: 488–492, 2007
35. Dickie P, Felser J, Eckhaus M, Bryant J, Silver J, Marinos N, Notkins AL: HIV-associated nephropathy in transgenic mice expressing HIV-1 genes. *Virology* 185: 109–119, 1991
36. Kopp JB, Klotman ME, Adler SH, Bruggeman LA, Dickie P, Marinos NJ, Eckhaus M, Bryant JL, Notkins AL, Klotman PE: Progressive glomerulosclerosis and enhanced renal accumulation of basement membrane components in mice transgenic for human immunodeficiency virus type 1 genes. *Proc Natl Acad Sci U S A* 89: 1577–1581, 1992
37. Kumar D, Plagov A, Yadav I, Torri DD, Sayeneni S, Sagar A, Rai P, Adabala M, Lederman R, Chandel N, Ding G, Malhotra A, Singhal PC: Inhibition of renin activity slows down the progression of HIV-associated nephropathy. *Am J Physiol Renal Physiol* 303: F711–F720, 2012
38. Shimizu A, Zhong J, Miyazaki Y, Hosoya T, Ichikawa I, Matsusaka T: ARB protects podocytes from HIV-1 nephropathy independently of podocyte AT1. *Nephrol Dial Transplant* 27: 3169–3175, 2012
39. D'Agati V: Pathologic classification of focal segmental glomerulosclerosis. *Semin Nephrol* 23: 117–134, 2003

This article contains supplemental material online at http://jasn.asnjournals.org/lookup/suppl/doi:10.1681/ASN.2012060590/-/DCSupplemental.